Supporting Information

One-dimensional Hybrid Copper Halides with High-Efficiency Photoluminescence as Scintillator

Zhongliang Gong[#,a], Jie Zhang[#,a,b], Ying-Yue Liu[a], Lu-Xin Zhang[a], Qing Zhang[a], Lingyun Xiao[a], Bingqiang Cao,[b,*] Bing Hu,[c,*] Xiao-Wu Lei[a,*]

[a] Research Institute of Optoelectronic Functional Materials, School of Chemistry, Chemical Engineering and Materials, Jining University, Qufu, Shandong, 273155, P. R. China

[b] School of Material Science and Engineering, University of Jinan, Jinan 250022, Shandong, China

[c] State Key Laboratory of Structural Chemistry, Fujian Institute of Research on the Structure of Matter, Chinese Academy of Sciences, Fuzhou, Fujian 350002, P. R. China, E-mail: hubing@fjirsm.ac.cn

Corresponding authors: Bingqiang Cao, Bing Hu, Xiao-Wu Lei

E-mail address: mse_caobq@ujn.edu.cn; hubing@fjirsm.ac.cn; xwlei_jnu@163.com

Experimental Section

Materials

All chemical reagents were purchased from the Aladdin chemical company. CuI (Aladdin), N-(3-Aminopropyl)cyclohexylamine (APCHA, 98%), HI (Aladdin, 55%-58%), Ethanol (AR, water ≤ 0.3%), Acetonitrile (Aladdin, ≥ 99.9%) and acetone (AR, 50 wt. % in H_2O).

Synthesis of [APCHA]Cu_2I_4:

A mixture of CuI (10 mmol, 1.904 g) and APCHA (5 mmol, 0.781 g) was dissolved in a mixture of HI (1 mL), ethanol (2 ml), and acetonitrile (3 ml). The suspension was stirred with constant heat for 10 min and then kept at room temperature. After 3 days of reaction, a large number of flaky white single crystals were filtered from the beaker and washed three times with ethanol. The structure was subsequently determined to be [APCHA]Cu_2I_4 ($C_9H_{22}Cu_2I_4N_2$) by single crystal X-ray diffraction. Elemental analysis calculated for $C_9H_{22}Cu_2I_4N_2$: C, 13.63%; N, 3.53%; H, 2.80%. Found: C, 13.28%; N, 3.62%; H, 2.25%.

Characterizations

The powder X-ray diffraction (PXRD) analysis was performed on a Bruker D8 ADVANCE powder X-ray diffractometer equipped with copper Ka radiation at a voltage of 40 kV and a current of 40 mA. The diffraction pattern was scanned over the angular range of 5-60 degrees (2θ) with a step size of 5° min^{-1} at room temperature. The thermogravimetric analysis (TG) was carried out on a Q600SDT thermogravimetric analyzer under both Air and N_2 atmosphere with a heating rate of 10 °C min^{-1} from 35 to 800 °C. The solid state UV-visible absorption spectra were obtained at room temperature by a PE Lambda 900 UV-visible spectrophotometer with $BaSO_4$ as the reference standard.

Single crystal X-ray diffraction

The single-crystal X-ray diffraction data of [APCHA]Cu_2I_4 was collected on a Bruker Apex II CCD diffractometer at 273 K. The crystal structures were solved and refined by the SHELXL-2018/3 program within OLEX2, with all atoms being refined with anisotropic atomic displacement parameters, except the H atoms, which were placed in idealized positions and allowed to ride on the relevant carbon atoms. Tables S1-S3 summarized the bond lengths, bond angles, and crystal refinement parameters of compounds [APCHA]Cu_2I_4. The Cambridge Crystallographic Data Centre (CCDC) 2361461 ($C_9H_{22}Cu_2I_4N_2$, 273 k).

Photoluminescence property characterizations

The photoluminescent excitation and emission spectra were recorded on an FLS980 spectrometer (Edinburgh) equipped with a continuous xenon lamp (450 W), and the photoluminescence quantum yield (PLQY) was achieved by incorporating an integrating sphere into the FLS980 spectrofluorometer. The PLQY was calculated according to the following formula: $\eta_{QE} = I_S/(E_R\text{-}E_S)$, where I_S represents the emission spectrum of the sample, E_R is the excitation spectrum of the empty integrating sphere without the sample, and E_S is the excitation spectrum of the sample. The PL decay curves were obtained upon excitation with an OPO pulsed laser (210-2400 nm, 10Hz, pulse width ≤5 ns, OPO TEK) at 300 nm and fitted by a single exponential function as follows: $I_{(t)} = I_0\, exp\,(-t/\tau)$, where I is the luminous intensity, t is the time after excitation, and τ is the lifetime of the exponential component. For temperature-dependent PL measurement, the samples were mounted on a thermal stage (77-873 K, THMS 600, Linkam Scientific Instruments). The E_a could be calculated according to the Arrhenius-type equation: $I_{PL} = I_0/[1+A\ \exp(-E_a/k_BT)]$, where I_{PL} and I_0 are the integrated emission intensities at a different temperature (T) and 0 K, respectively, and k_B is the

Boltzmann constant. The S could be calculated according to the following formula:

$$FWHM = 2.36\sqrt{S}\hbar\omega_{photon}\sqrt{coth\frac{\hbar\omega_{photon}}{2k_BT}}$$

Where the S and $\hbar\omega_{photon}$ represent the electron-phonon coupling strength and phonon frequency, respectively. The CIE chromaticity coordinates were determined based on the emission spectra.

X-Ray Property Characterization

RL properties were investigated on an X-ray source-equipped fluorescence spectrometer. The Hamamatsu R928 PMT was used to detect the X-ray response intensity. A commercially available LuAG: Ce was utilized as a reference to evaluate the scintillation light yield. The light yield was estimated using the following equation:

$$\frac{LY_{sample}}{LY_{LuAG:\,Ce}} = \frac{R_{sample}}{R_{LuAG:\,Ce}} \times \frac{\int I_{LuAG:\,Ce}(\lambda)/S(\lambda) \int I_{LuAG:Ce}(\lambda)d\lambda}{\int I_{sample}(\lambda)/S(\lambda) \int I_{sample}(\lambda)d\lambda}$$

Where R is defined as the X-ray deposited energy percentage of scintillators, $I(\lambda)$ is the radioluminescence spectrum at different wavelengths, and $S(\lambda)$ represents the detection efficiency at different irradiation areas, respectively. The absorption coefficient (α) is mainly determined by atomic number (Z_{eff}) with the equation of $\alpha \propto \rho Z_{eff}^4/E^3$, where ρ and E are mass density and X-ray photon energy, respectively. The MTF value is defined by the Fourier transform of the LSF as follows:

$$MTF(v) = F(LSF(x)) = F(\frac{dESF(x)}{dx})$$

Where ν is the spatial frequency, and x is the position of the pixels.

Calculation of the Detection Limit

The detection limit is the lowest detectable dose rate of an X-ray scintillator. We tested and recorded the RL intensity of $[APCHA]Cu_2I_4$ at low dose rates of 2-50 μGy_{air} s^{-1} and obtained the corresponding fitting curves based on measured data. The detection limit is defined by the International Union of

Pure and Applied Chemistry (IUPAC) as the equivalent dose rate (signal-to-noise ratio [SNR] = 3) that produces a signal greater than three times the noise level, and the detection limit of [APCHA]Cu_2I_4 is derived from its fitted curve to the value at an SNR of three. The formula is as follows: LOD = $3\sigma/k$, where σ represents the background noise of the instrument and k represents the absolute value of the slope of the fitted curve.

Preparation of the PDMS Thin Film with [APCHA]Cu_2I_4

The thin film was prepared by a spin coating method on the quartz plate. At first, the [APCHA]Cu_2I_4 powder was sonicated and dispersed in CH_2Cl_2. Then, the PDMS prepolymer was well-mixed with the [APCHA]Cu_2I_4 followed by a vacuuming process for 5 minutes to remove air and CH_2Cl_2 from PDMS. The mixture was spun coating on the quartz plate uniformly. Finally, the thin film was prepared by heat treatment at 80 °C for one hour.

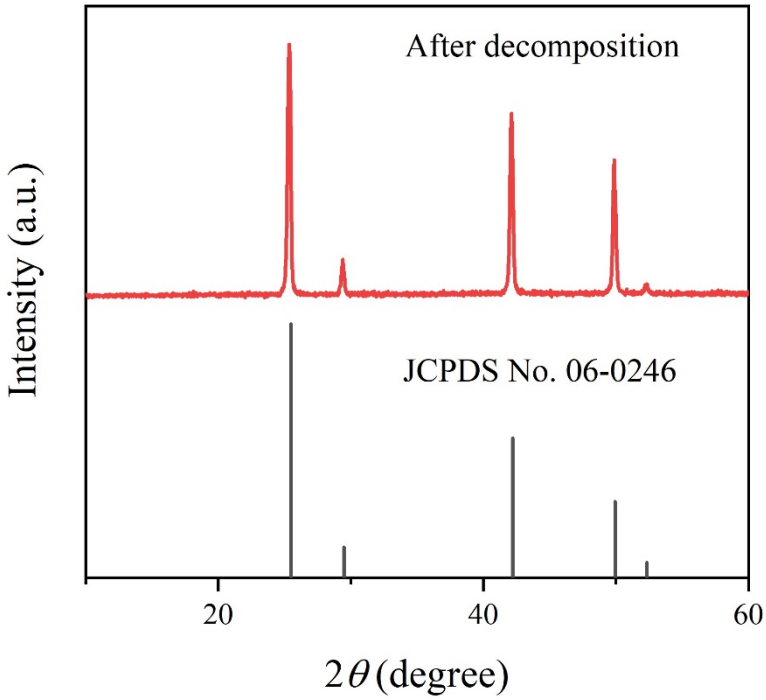

Fig. S1 The XRD pattern of [APCHA]Cu_2I_4 after decomposition at 420 °C and the JCPDS card (No. 06-0246) of CuI.

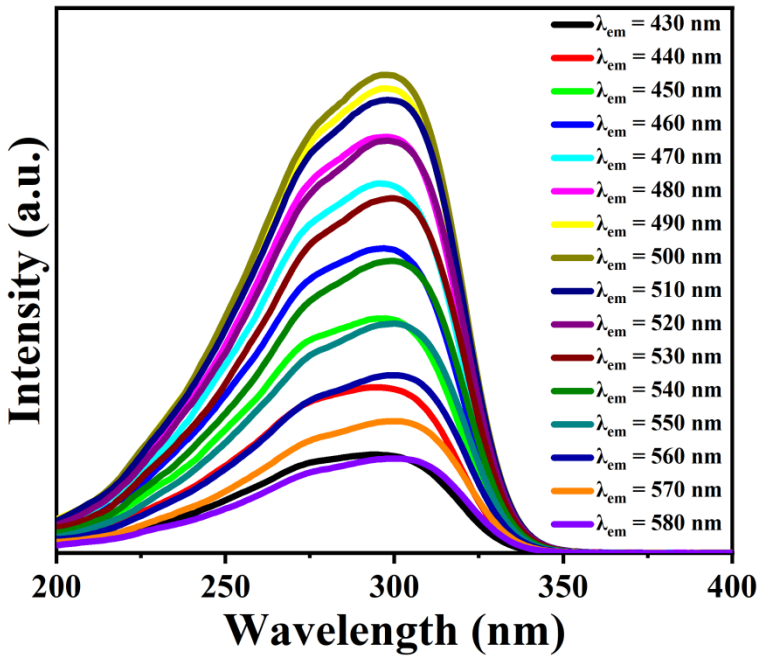

(a)

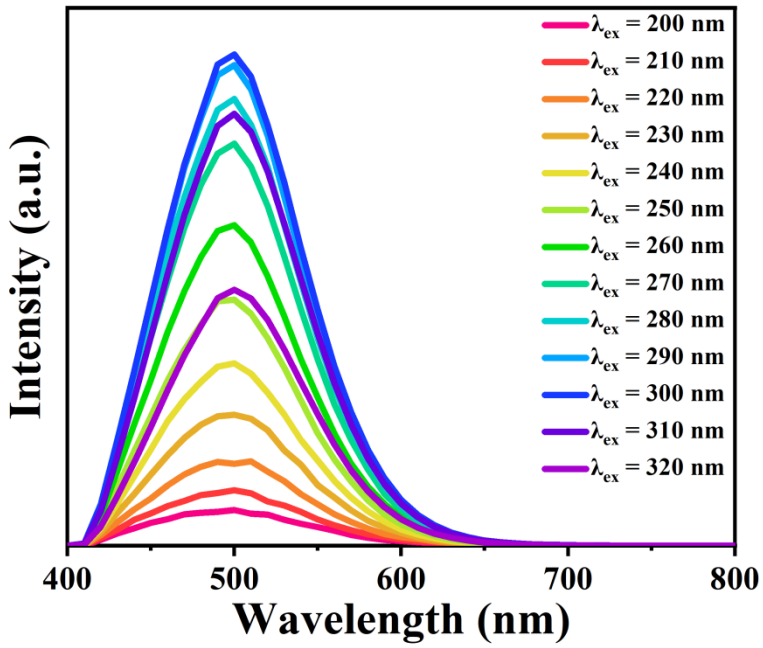

(b)

Fig. S2 The emission wavelength-dependent PL excitation spectrum (a) and excitation wavelength-dependent PL emission spectrum (b) of [APCHA]Cu_2I_4.

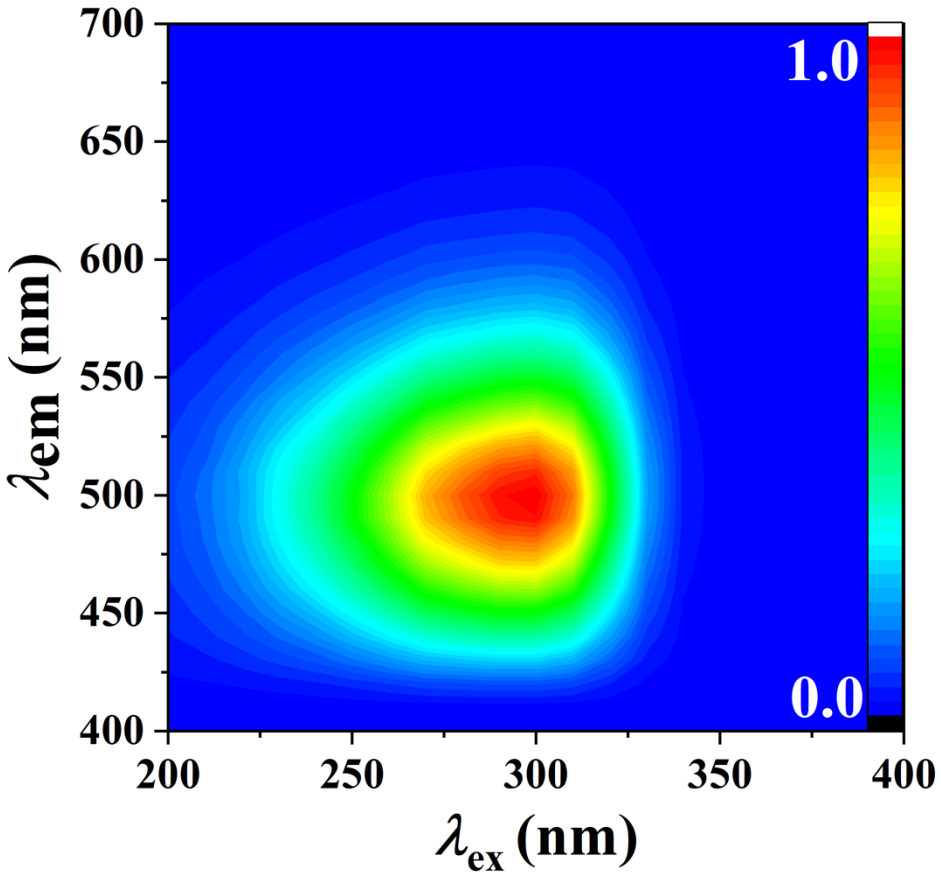

Fig. S3 Contour plot of the PL emission spectra collected as a function of excitation wavelength for [APCHA]Cu_2I_4.

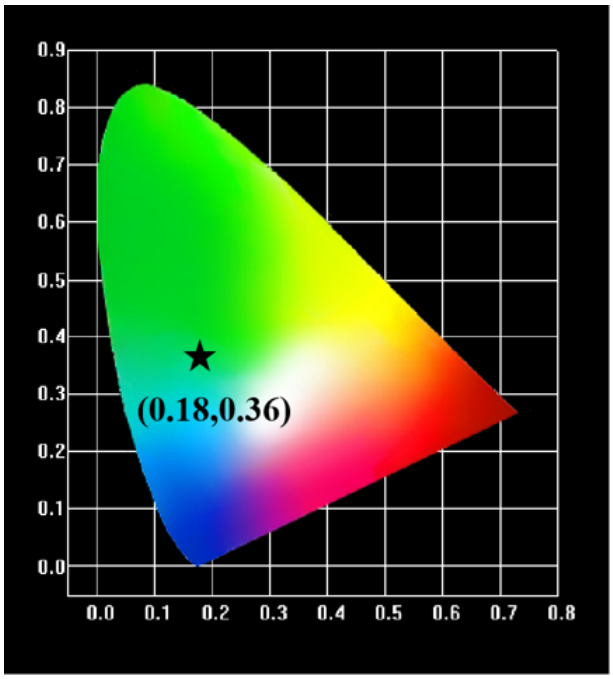

Fig. S4 The CIE chromaticity coordinates of [APCHA]Cu_2I_4.

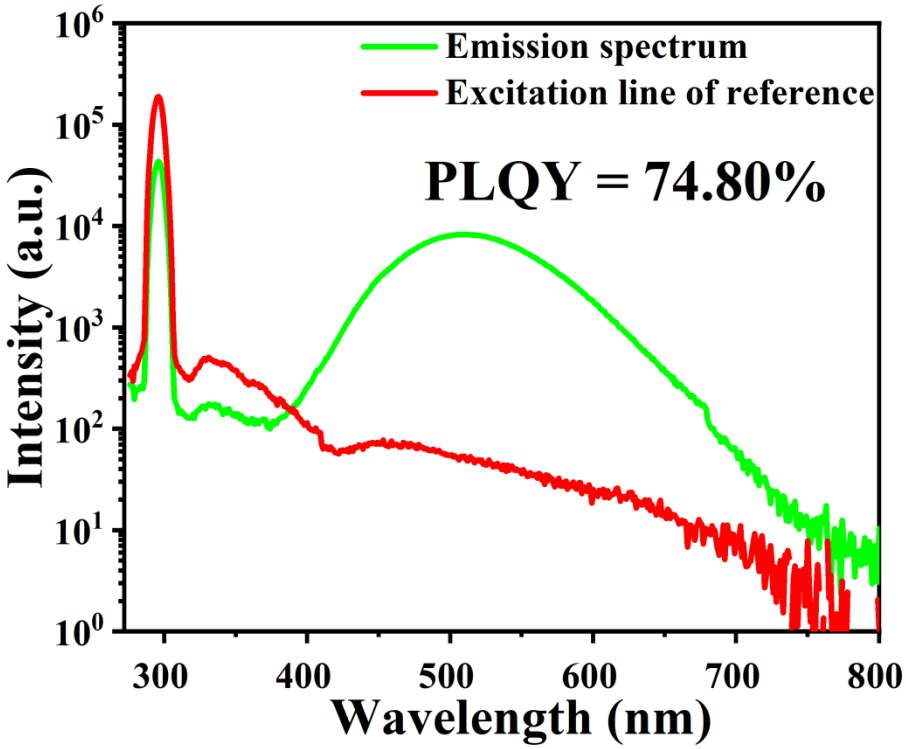

Fig. S5 The PLQY of bulk crystals for compound [APCHA]Cu_2I_4.

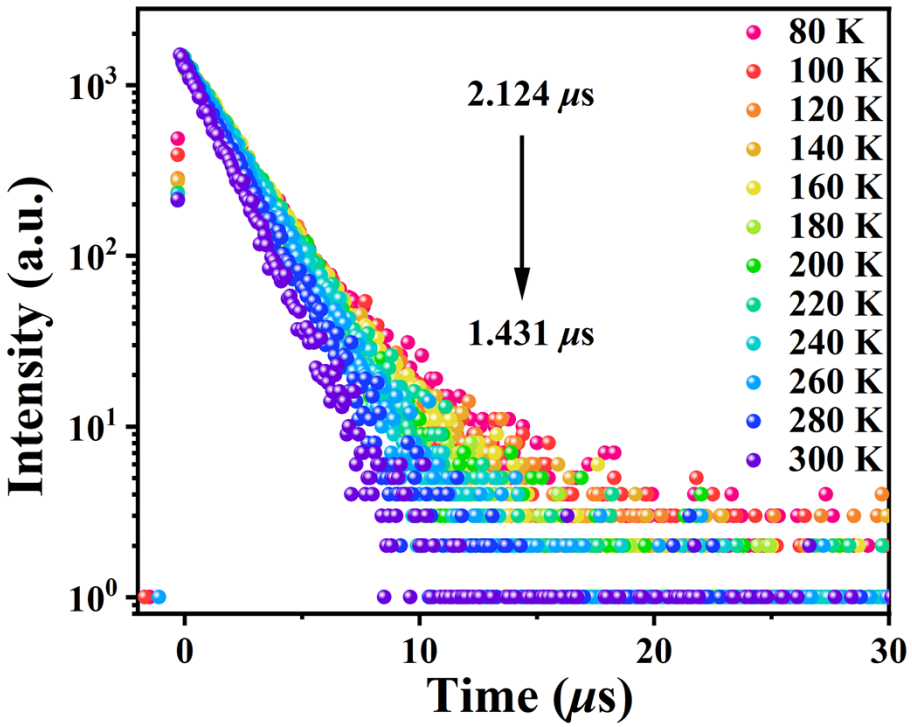

Fig. S6 Temperature-dependent PL decay curves (λ_{ex} = 296 nm, λ_{em} = 498 nm) of the halide.

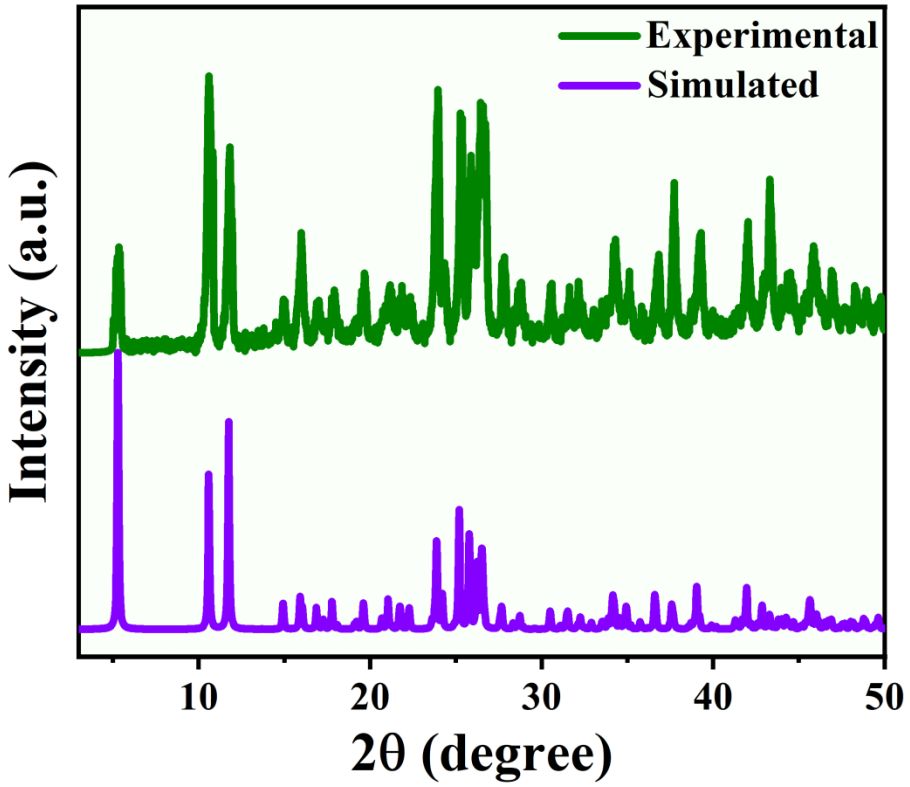

Fig. S7 The PXRD pattern of [APCHA]Cu_2I_4 after being stored in the air for 2 months.

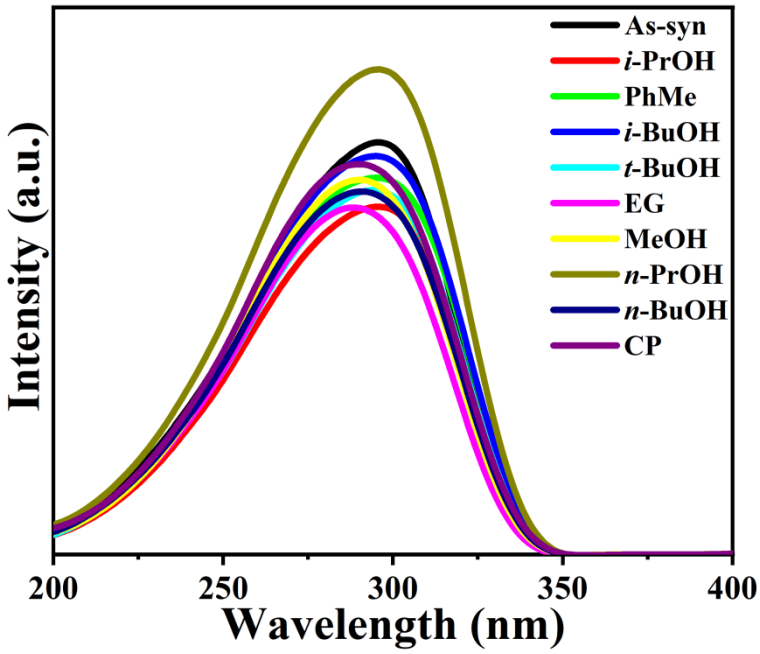

(a)

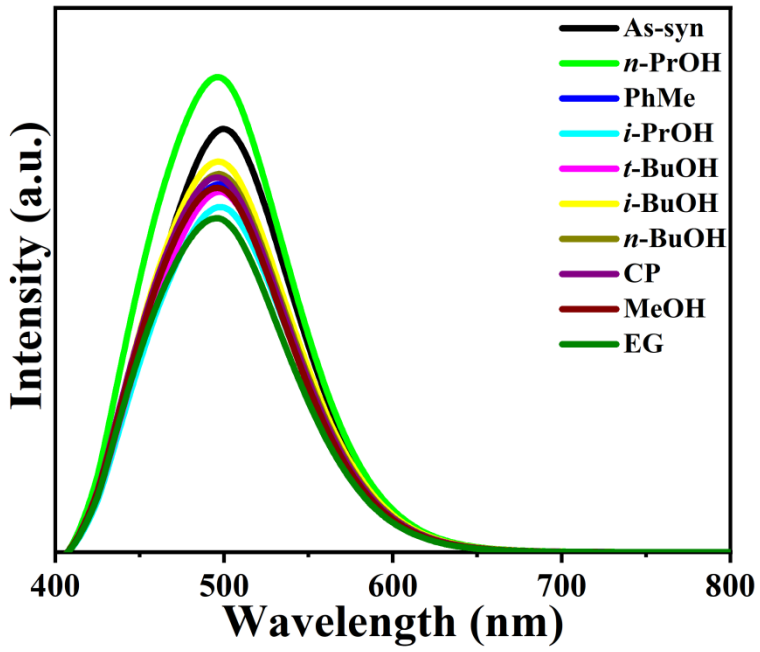

(b)

Fig. S8 The PL excitation (a) and emission (b) spectra of [APCHA]Cu_2I_4 after soaking in various organic solvents over one day (*i*-PrOH = Isopropanol, PhMe = Methylbenzene, *i*-BuOH = Isobutanol, *t*-BuOH = Tert-Butanol, EG = Ethylene glycol, MeOH = Methanol, *n*-PrOH = n-propanol, *n*-BuOH = n-Butanol, CP = Acetone).

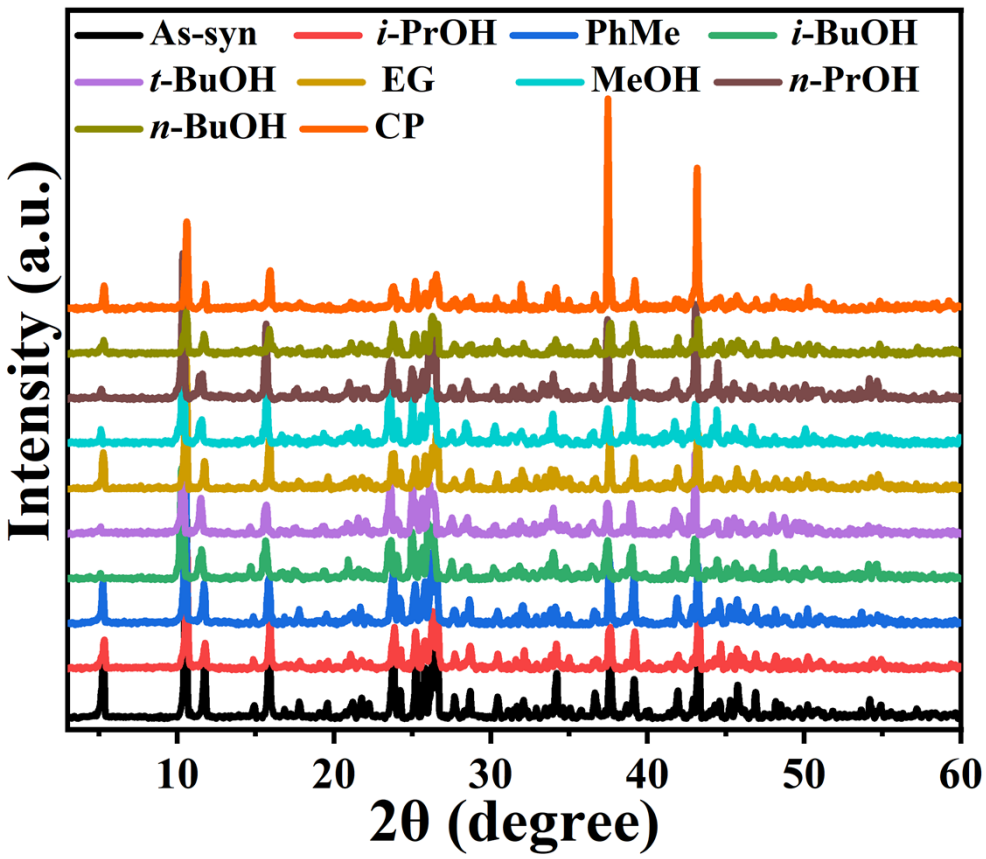

Fig. S9 The XRD spectra of [APCHA]Cu_2I_4 after soaking in various organic solvents over one day (*i*-PrOH = Isopropanol, PhMe = Methylbenzene, *i*-BuOH = Isobutanol, *t*-BuOH = Tert-Butanol, EG = Ethylene glycol, MeOH = Methanol, *n*-PrOH = n-propanol, *n*-BuOH = n-Butanol, CP = Acetone).

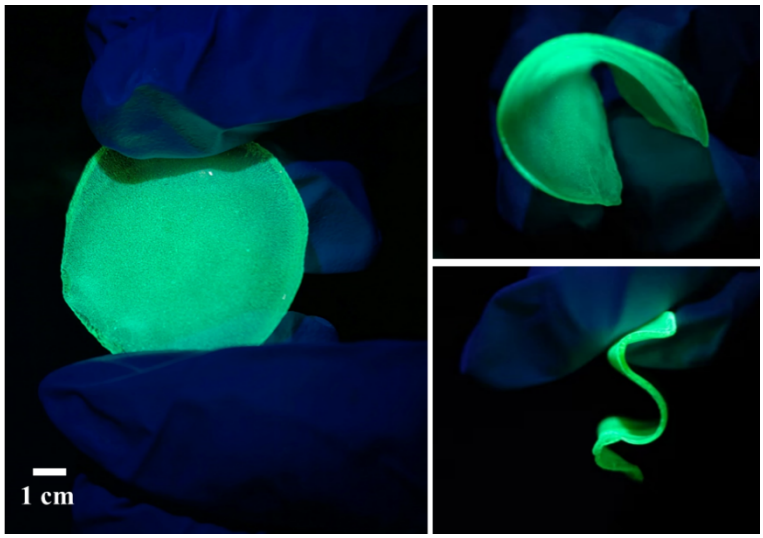

Fig. S10 Photos of the [APCHA]Cu_2I_4-based flexible film under the 365 nm UV light (the scale bar = 1 cm).

Table S1. Crystal Data and Structural Refinements for [APCHA]Cu_2I_4.

Compound	[APCHA]Cu_2I_4
chemical formula	$C_9N_2H_{22}Cu_2I_4$
Fw	792.96
Space group	$P2_1$ (No. 4)
crystal system	monoclinic
a/Å	6.7267(2)
b/Å	8.4253(3)
c/Å	16.8186(6)
α/°	90
β/°	96.1730(10)
γ/°	90
V(Å^3)	947.66(6)
Z	2
D_{calcd} (g·cm^{-3})	2.779
Temp (K)	273
μ (mm^{-1})	8.745
F(000)	720.0
Reflections collected	9623
Unique reflections	4339
GOF on F^2	1.049
R_1,wR_2 ($I > 2\sigma(I)$)[a]	0.0304/0.0668
R_1,wR_2 (all data)	0.0344/0.0688
$\Delta\rho_{max}$ (e/Å^3)	1.80
$\Delta\rho_{min}$ (e/Å^3)	-1.78

[a] $R_1 = \sum||F_o| - |F_c||/\sum|F_o|$, $wR_2 = \{\sum w[(F_o)^2 - (F_c)^2]^2/\sum w[(F_o)^2]^2\}^{1/2}$

Table S2. Selected bond lengths (Å) and bond angles (°) for [APCHA]Cu_2I_4.

Cu1-I1	2.743(6)	Cu1-I2	2.593(10)
Cu1-I3[1]	2.707(12)	Cu1-I4[1]	2.705(11)
Cu2-I1	2.809(2)	Cu2-I2	2.5780(16)
Cu2-I3	2.6317(16)	Cu2-I4	2.6814(16)
I1-Cu1-I2	104.4(3)	I1-Cu1-I3[1]	110.5(4)
I1-Cu1-I4[1]	112.6(4)	I2-Cu1-I3[1]	115.1(4)
I2-Cu1-I4[1]	115.7(4)	I3[1]-Cu1-I4[1]	98.7(3)
I1-Cu1A-I2	96.5(3)	I1-Cu1A-I3[1]	103.8(2)
I1-Cu1A-I4[1]	105.8(2)	I2-Cu1A-I3[1]	121.0(2)
I2-Cu1A-I4[1]	121.8(2)	I3[1]-Cu1A-I4[1]	104.9(2)
I1-Cu2-I2	102.96(6)	I1-Cu1-I3	104.12(6)
I1-Cu1-I4	109.63(6)	I2-Cu1-I3	116.61(7)
I2-Cu1-I4	121.12(7)	I3-Cu1-I4	101.27(5)
Cu1-I1-Cu2	73.0(2)	Cu1A-I1-Cu2	73.28(7)
Cu1-I2-Cu2	79.37(14)	Cu1A-I2-Cu2	86.9(2)
Cu1[2]-I3-Cu2	79.9(2)	Cu1A[2]-I3-Cu2	75.74(16)
Cu1[2]-I4-Cu2	79.1(2)		

[#1]-1+*x*, +*y*, +*z*; [#2]1+*x*, +*y*, +*z*

Table S3. Hydrogen bonds data for [APCHA]Cu_2I_4.

D-H···A	d(D-H)	d(H···A)	d(D···A)	<(DHA)
N1-H1A···I1	0.89	2.88	3.614(7)	140
N1-H1B···I1	0.89	2.74	3.594(7)	161
N1-H1C···I1	0.89	2.99	3.756(7)	145
N2-H2A···I3	0.89	2.97	3.673(6)	137
N2-H2A···I4	0.89	3.06	3.665(6)	127
N2-H2B···I2	0.89	2.85	3.738(7)	175

Table S4. Temperature-dependent PL peak wavelength and lifetime of the [APCHA]Cu_2I_4.

Temperature (K)	Peak wavelength (nm)	Lifetime (μs)
80	506	2.124
100	506	2.068
120	510	2.038
140	510	2.026
160	508	2.018
180	503	1.931
200	508	1.916
220	501	1.916
240	506	1.881
260	503	1.801
280	498	1.657
300	501	1.431